# Influence of Carbon Nanotubes with Different Functional Groups on the Morphology and Properties of PPO/PA6 Blends

**Yu Shen,[1,2] Zhenghong Guo,[2] Jie Cheng,[2] Zhengping Fang[1,2]**

[1]*Institute of Polymer Composites, Zhejiang University/MOE Key Laboratory of Macromolecular Synthesis and Functionalization, Hangzhou 310027, China*
[2]*Lab of Polymer Materials and Engineering, Ningbo Institute of Technology, Zhejiang University, Ningbo 315100, China*

Received 27 July 2009; accepted 2 October 2009
DOI 10.1002/app.31540
Published online 23 December 2009 in Wiley InterScience (www.interscience.wiley.com).

**ABSTRACT:** Carbon nanotubes with different functional groups were prepared and then incorporated into the poly(2,6-dimethyl-1,4-phenylene oxide)/polyamide 6 (PPO/PA6) blend via melt blending. The influence of different carbon nanotubes on the morphology and properties of the blend was studied. The results show that addition of pristine CNTs, CNTs-OH, CNTs-$NH_2$ leads to the evolution of the phase structure of PPO/PA6 (mass ratio: 60/40) blend from sea-island to cocontinuous, whereas incorporation of CNTs-COOH does not change the blend morphology due to serious aggregation of the carbon nanotubes. Incorporating different CNTs into PPO/PA6 blend increases the tensile modulus and storage modulus of the blends, whereas decreases slightly the tensile strength. At the same time, the glass transition temperatures ($T_g$) of PA6 and PPO are enhanced. $\Delta T_g$, the gap between the $T_g$ of PA6 and PPO, decreases with the addition of carbon nanotubes due to the stronger interaction of carbon nanotubes with PA6 than PPO. A similar tendency was found in the storage modulus ($G'$) and complex viscosity ($\eta^*$) of the composites. The dispersion state of different carbon nanotubes and their interaction with polymer components are different, which causes the different confinement effect to the macromolecular chains. © 2009 Wiley Periodicals, Inc. J Appl Polym Sci 116: 1322–1328, 2010

**Key words:** carbon nanotubes; polyamide; polyphenylene oxide; blend; nanocomposites

## INTRODUCTION

Poly(2,6-dimethyl-1,4-phenylene oxide)/polyamide 6 (PPO/PA6) blends combine the advantages of dimension stability and heat resistance of PPO and chemical resistance and low melt viscosity of PA6. Since the first commercialization by GE plastics in 1984, PPO/PA6 blends have attracted much attention by both academic and commercial fields. However, PPO/PA6 blends are typical incompatible systems. Their properties are strongly dependant on the morphology and interfacial adhesion of the two phases. Consequently, many studies have reportedly improved the compatibility of PPO/PA6 blends by grafting functional monomers onto PPO and/or PA6 components.[1–5] For example, the anionic ring-opening polymerization of ε-caprolactam was carried out in the presence of PPO, the chain of which bore p-methoxyphenylpropionate, acting as macroactivator to initiate PA6 chain growth from the PPO chain and form a graft copolymer of PPO and PA6 and pure PA6 simultaneously.[6,7]

The effect of nanoparticles on the morphology and properties of polymer blends has attracted great interest because of the improved physical properties compared with unmodified polymers. Organically modified montmorillonite was introduced into a PPO/ABS system and the fabricated cocontinuous nanocomposites showed greatly improved mechanical properties over the whole temperature range.[8] With the addition of organoclay into PPO/PA6 blends, the matrix-domain structure transforms into the cocontinuous morphology due to the selective localization of clay in the PA6 phase which changes the viscosity ratio of the PPO and PA6 phases and the high aspect ratio of the clay platelets prevents the coalescence of domains during melt mixing.[9] The PPO/PA6/epoxycyclohexyl polyhedral oligomeric silsesquioxane (POSS) composites with cocontinuous morphology have better mechanical properties than those with droplet/matrix morphology and the epoxycyclohexyl POSS acts as a chain extender and a crosslinking agent for PA6.[10]

*Correspondence to:* Z. Fang (zpfang@zju.edu.cn).
Contract grant sponsor: Natural Science Foundation; contract grant number: 50873092.

Carbon nanotubes (CNTs) have been extensively studied because of their excellent mechanical, electrical, and thermal properties, which make them an ideal candidate as reinforcing fillers. It is reported that CNTs can enhance the phase dispersion of polymer blends.[11] The addition of CNTs in the PVDF/PA blends significantly increases the melt viscosity of PA6 phase, and a phase transformation from sea-island to cocontinuous occurs upon adding more than 1.2 wt % CNTs into the blends.[12] Modification of CNTs improves their dispersion in a polymer matrix and affects the properties of polypropylene/ethylene-*co*-vinyl acetate blends[13] and UHMWPE/HDPE blends.[14] Collister reported[15] that carbon nanotubes-based PPO/PA nanocomposites are commercially attractive because of the improvements in strength and modulus, improved thermal durability, reduced permeability, improved electrical properties, and improved flame resistance. These properties are improved with minimal sacrifice to the ductility and impact resistance. These property modifications are achieved at low loading levels (2 to 5 wt %), and this has minimal effects on the mass and costs of the compounded materials. However, there are very few detailed studies on PPO/PA systems filled with CNTs and functionalized CNTs.

This work aims to investigate the effects of CNTs with different functional groups, namely pristine CNTs, acid-modified CNTs (CNTs-COOH), hydroxy-modified CNTs (CNTs-OH), and diamine-modified CNTs (CNTs-$NH_2$) on the morphology, tensile properties, dynamic mechanical properties, and viscoelastic behavior of PPO/PA6 blends. Furthermore, the morphology evolution of PPO/PA6/CNTs (CNTs-COOH, CNTs-OH, and CNTs-$NH_2$) blends are also discussed.

## EXPERIMENTAL

### Materials

Poly(2,6-dimethyl-1,4-phenylene oxide) (PPO, code Noryl 731) was obtained from Sabic GE Plastics Co. USA, with the $\overline{M}_w$ of 605,000 g/mol (determined by gel permeation chromatography, GPC). Polyamide 6 (PA6, code CM1017) was produced by Toyolac, Japan, with the $\overline{M}_w$ of 627,000 g/mol (determined by GPC). Carbon nanotubes (CNTs), with an average diameter of 20 ± 5 nm and a length of 1–10 μm, were prepared by catalytic chemical vapor deposition (CCVD) method and provided by Chengdu Organic Chemicals Co. (Chengdu, China).

### Preparation of functionalized carbon nanotubes

Different functionalized CNTs (CNT-x) were prepared using the following procedures.

*CNTs-OH*: 100 mg CNTs, 5 g KOH, and 100 mL ethanol were first sonicated for 30 min, then reacted for 8 h under reflux temperatures while stirring. The product was filtered and washed three times with ethanol, followed by washing with deionized water until the filtrated liquor was neutral. The residue was dried in a vacuum oven under 80°C for 12 h to obtain hydroxylated carbon nanotubes (CNTs-OH).

*CNTs-$NH_2$*: 50 mg CNTs-OH was predispersed in 50 mL toluene by sonicating for 30 min, and heated to 80°C with stirring. Then, excess amount of amino-silane/toluene mixture was dropped slowly and reacted under this temperature for 8 h. The product was filtered and washed with toluene, ethanol, and deionized water, three times for each liquid, until the filtrated liquor was neutral. The residue was dried in a vacuum oven under 80°C for 12 h to obtain amino-functionalized carbon nanotubes (CNTs-$NH_2$).

*CNTs-COOH*: 2 g CNTs was added into 200 mL of 3 : 1 (vol %) mixture of sulfuric acid (98 vol %) and nitric acid (68 vol %), sonicated for 30 min at room temperature, then heated to reflux for 8 h. The resultant solid was filtered and washed with deionized water a minimum of 10 times, until the filtrated liquor was neutral. The residue was dried in a vacuum oven under 80°C for 12 h to obtain carboxylated carbon nanotubes (CNTs-COOH).

### Composites preparation

Before blending, PPO and PA6 were dried at 85°C under vacuum for about 12 h. PPO, PA6, and different carbon nanotubes were reactively blended in the mixing chamber of a Thermohaake rheomixer (Haake Torque Rheometer, model Polydrive) at 240°C and 70 rpm for 10 min. The composites were compression molded in a press at 240°C for 20 min, then cold pressed to obtain samples for testing.

### Characterization

Fourier transform infrared spectra (FTIR) of different carbon nanotubes were recorded on a Bruker Vector 22 spectrometer, using KBr pellets. Characteristic absorption peaks of hydroxyl, amino, carboxyl groups were observed to determine the structure of CNT-x.

Thermogravimetric analysis (TGA) was performed on a TA STD Q600 thermal analyzer at a heating rate of 10°C/min, in nitrogen atmosphere, with a scan range of 50 to 650°C.

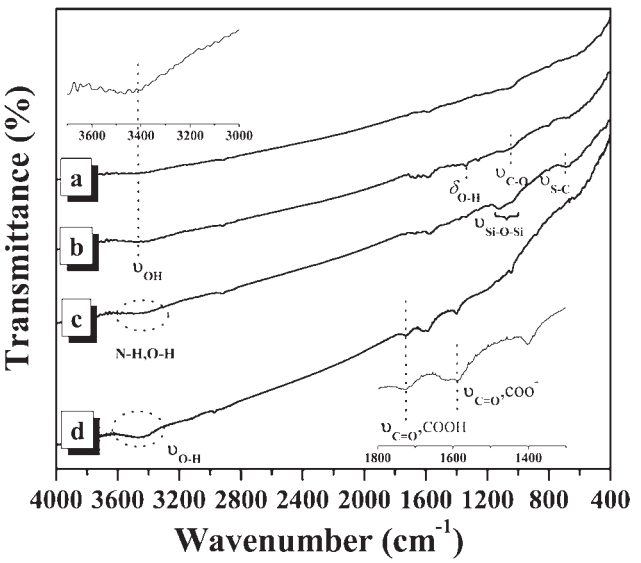


**Figure 1** FTIR spectra of (a) pristine CNTs, (b) CNTs-OH, (c) CNTs-$NH_2$, and (d) CNTs-COOH.

An S-570 scanning electron microscope (SEM) was used to study the morphology of PPO/PA6 blends. Samples were etched with toluene, a good solvent for PPO, before observation. The impact fracture surfaces were coated with a layer of gold to avoid electrical charging and to increase image contrast.

Tensile tests were carried out on a tensile tester (model WDW-10). The specimens were prepared according to GB1040-89 (similar to ISO527-1993). The crosshead speed was 50 mm/min and the gage length was 50 mm. All the tests were performed at 23°C. The results of five measurements for each sample were averaged.

Dynamic mechanical analysis (DMA) was performed on a DMA242C dynamic mechanical analyzer, with a specimen dimension of 16 × 12 × 1.4 mm. A temperature range of 0 to 200°C at a heating rate of 3°C/min and a frequency of 1 Hz was used after optimization of the static and dynamic loads.

Rheological properties of PPO/PA6 and its nanocomposites were conducted on a controlled strain rate rheometer (ARES rheometer) in an air environment and the size of samples measured was 25 mm in diameter and with a gap of 1.1 mm. Frequency sweeping was performed at 240°C at a frequency range of 0.01 to 100 $s^{-1}$, with a strain of 1% to ensure the materials were in the linear viscosity range.

## RESULTS AND DISCUSSION

The IR spectra of pristine CNTs, CNTs-OH, CNTs-$NH_2$, and CNTs-COOH are shown in Figure 1. Pristine CNTs have no any characteristic absorption peaks in the wave number range studied. CNTs-OH show characteristic —OH peaks at about 3440 $cm^{-1}$ and 1338 $cm^{-1}$ due to the O—H stretching and bending, respectively, and about 1050 $cm^{-1}$ (wide peak) due to the C—O stretching, indicating that presence of —OH groups in CNTs. For CNTs-$NH_2$, the absorption peaks at high wave number does not change significantly due to the superposition of the absorption peaks of —OH and —$NH_2$. However, a new peak at 1000–1160 $cm^{-1}$ appears which is attributed to Si—O—Si, suggesting that a condensation reaction takes place between silane groups. At the same time, the absorption at 680 $cm^{-1}$ is due to the stretching of the Si—C bond and the appearance of these new peaks reveals the introduction of amino silane onto CNTs. For CNTs-COOH, the absorption peaks at 3440 $cm^{-1}$ (attributed to the stretching of O—H), 1720 $cm^{-1}$ (attributed to the stretching of C=O), 1580 $cm^{-1}$ (attributed to the reverse symmetric stretching of $COO^-$), and 1400 $cm^{-1}$ (attributed to the bending of O—H in COOH) all indicate that the carboxyl groups have been introduced onto the surface of CNTs.

Thermogravimetric analysis is often used to characterize the structural changes of CNTs, and in particular, the amount of functional groups bonded on the CNT skeleton. Figure 2 shows the thermogravimetric curves of pristine CNTs, CNTs-OH, CNTs-$NH_2$, and CNTs-COOH in nitrogen atmosphere. Pure CNTs do not degrade in nitrogen, with a 99.3 wt % residue at 600°C. The CNTs-OH start to degrade at about 155°C with a 97.6 wt % residue at 600°C. The residue of CNTs-$NH_2$ is only 86.8 wt %, with the increased weight loss possibly due to the debonding of amino silane from CNTs. For CNTs-COOH, weight loss starts below 100°C, which may be due to the degradation of carboxyl groups. Furthermore, treatment with concentrated acid at high

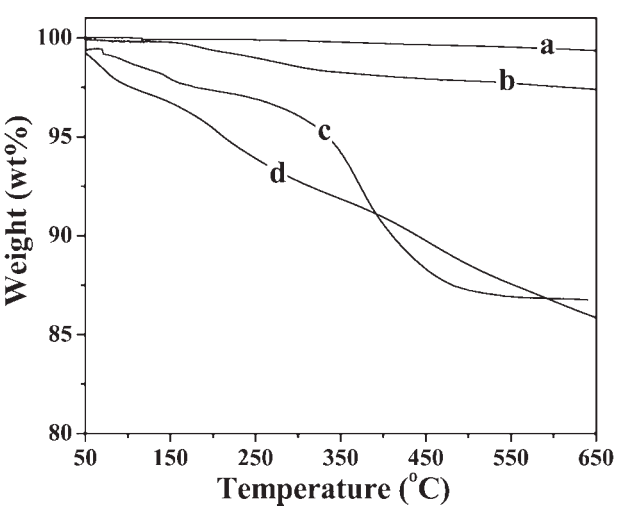


**Figure 2** TGA curves of (a) pristine CNTs, (b) CNTs-OH, (c) CNTs-$NH_2$, and (d) CNTs-COOH.

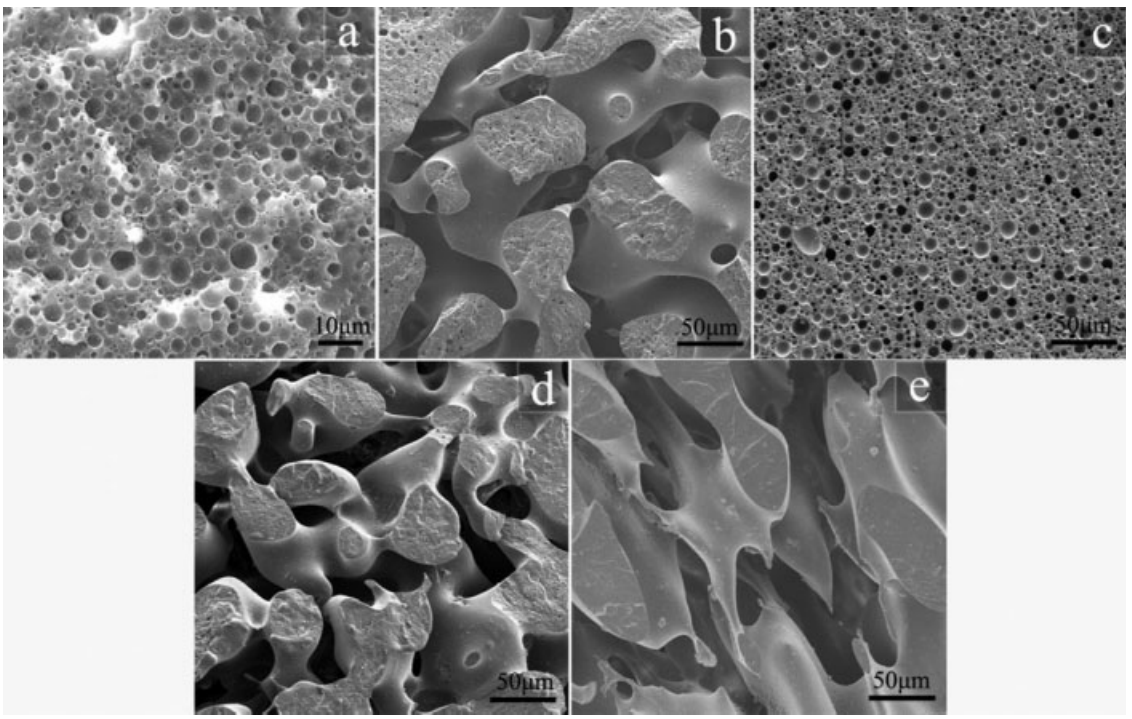


**Figure 3** SEM images of toluene etched PPO/PA6/CNTs (60/40/1): (a) without CNTs (b) pristine CNTs, (c) CNTs-COOH, (d) CNTs-OH, and (e) CNTs-$NH_2$.

temperatures can destroy the regular structure of CNTs, resulting in a loss of thermal stability of carbon nanotubes. In short, more the functional groups, more is the weight loss.

Figure 3 shows SEM observation of the PPO/PA6(60/40) blend and its composites with different CNTs. Samples were etched with toluene, a good solvent for PPO, before observation. The PPO/

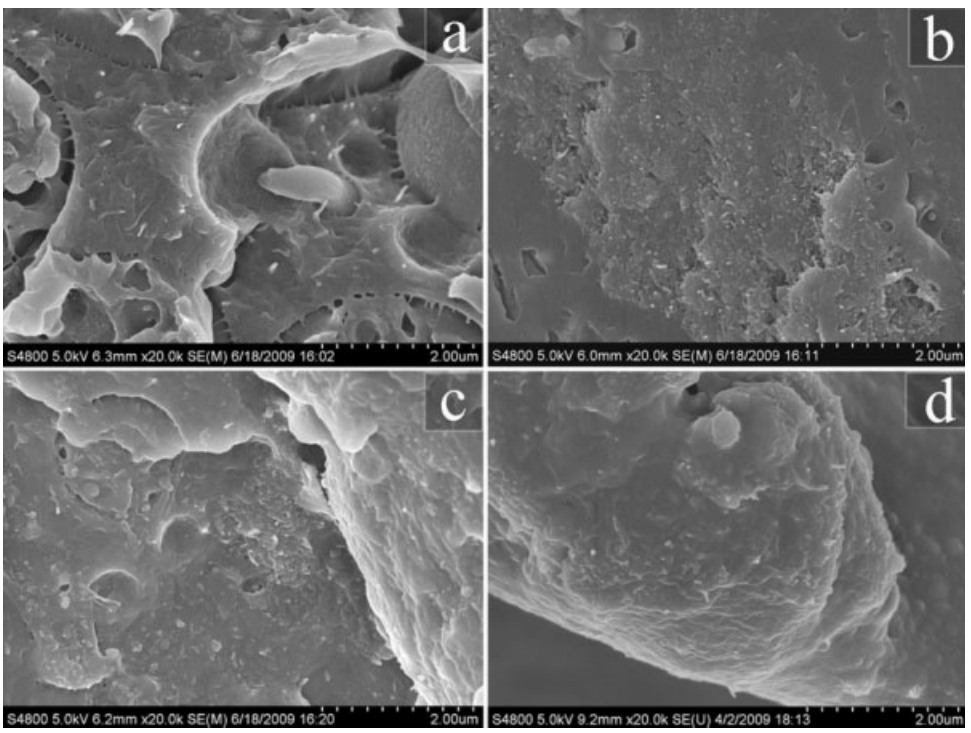


**Figure 4** SEM images of the impact fracture surface of PPO/PA6/CNTs (60/40/1): (a) pristine CNTs, (b) CNTs-COOH, (c) CNTs-OH, and (d) CNTs-$NH_2$.

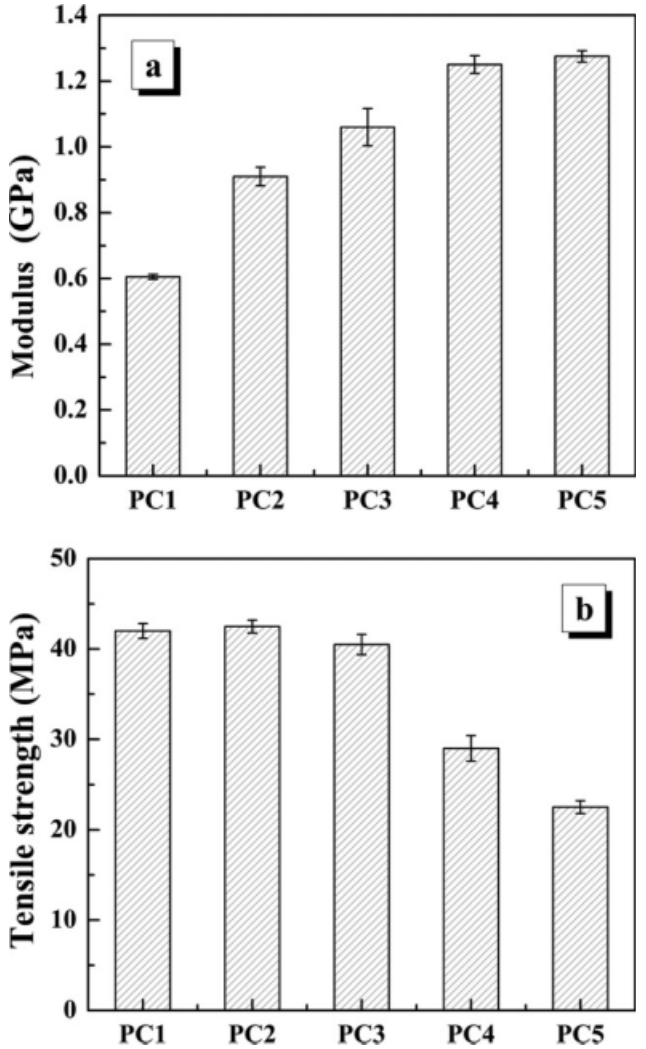


**Figure 5** Tensile modulus (a) and strength (b) of (PC1) PPO/PA6 (60/40), (PC2) PPO/PA6/ pristine CNTs (60/40/1), (PC3) PPO/PA6/CNTs-COOH (60/40/1), (PC4) PPO/PA6/CNTs-OH(60/40/1), and (PC5) PPO/PA6/CNTs-$NH_2$ (60/40/1).

PA6(60/40) blend shows a typical sea-island structure, with dispersed PPO (having higher melt viscosity) phase and continuous PA6 (having lower melt viscosity) phase. Addition of different CNTs resulted in various changes to the morphology of the blend. Adding CNTs-COOH did not significantly change the morphology [Fig. 3(b)]; whereas adding CNTs, CNTs-OH, and CNTs-$NH_2$ [Fig. 3(a,c,d)] resulted in a change of the morphology from sea-island to cocontinuous structures. This result can be explained by the influence of CNTs on the melt viscosity of the component polymers. The CNTs, CNTs-OH, and CNTs-$NH_2$ are selectively distributed in the PA6 phase, constraining the PA6 chain motions and thus increasing the melt viscosity of PA6.[12] When the melt viscosity of PA6/CNTs phase is equivalent to that of PPO, the morphology of the composites transforms from sea-island to cocontinuous structures. For CNTs-COOH, however, the confinement effect is reduced due to the significant shortening of the tubes that occurs during acid treatment.[16,17] Consequently, the morphology of PPO/PA6/CNTs-COOH remains unchanged.

To investigate the dispersion of different CNTs in the PPO/PA6(60/40) blend, the fractured surfaces were observed with SEM, as shown in Figure 4. The dispersion appears significantly different for the range of CNTs studied. Pure CNTs are dispersed homogeneously in the blend, with very few aggregates while there are some aggregates in the composites containing CNTs-OH and CNTs-$NH_2$. It is notable that many compact aggregates are found in PPO/PA6/CNTs-COOH composites and this phenomenon is most probably caused by the strong interaction between high polar carboxyl groups.[18] Another possible reason is the esterification that

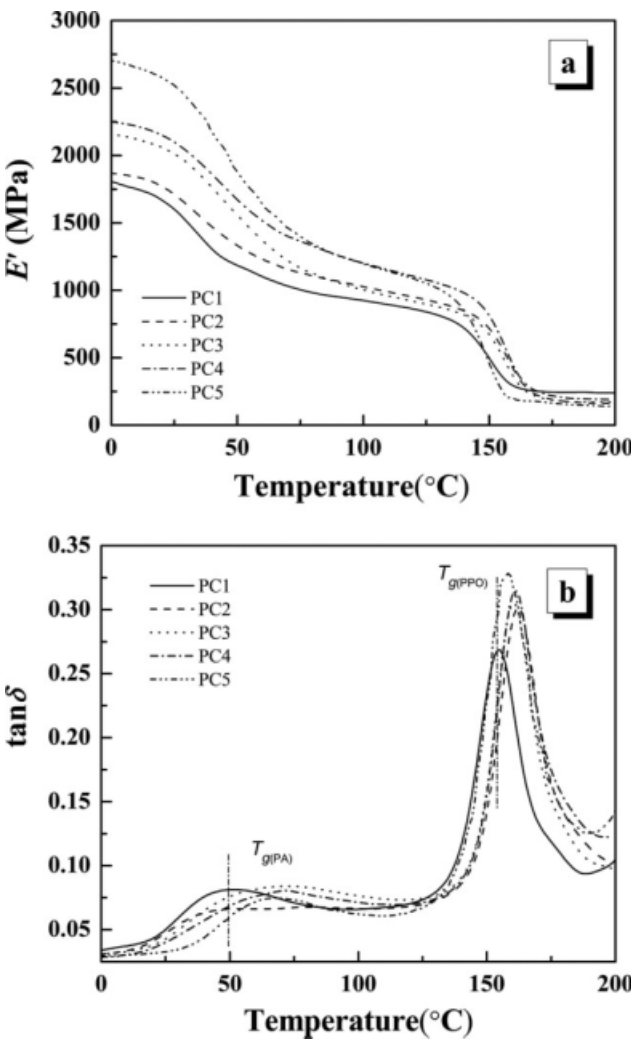


**Figure 6** Storage modulus ($E'$) and loss tangent (tan δ) of (PC1) PPO/PA6 (60/40), (PC2) PPO/PA6/pristine CNTs (60/40/1), (PC3) PPO/PA6/CNTs-COOH (60/40/1), (PC4) PPO/PA6/CNTs-OH (60/40/1), and (PC5) PPO/PA6/CNTs-$NH_2$ (60/40/1).

**TABLE I**
**The Results of DMA Analysis for PPO/PA6/CNTs-x (60/40/1) Composites**

| Sample | $E'$ (MPa)[a] | $T_g$ (°C) | | $\Delta T_g$ (°C) |
|---|---|---|---|---|
| | | PA6 | PPO | |
| PC1–PPO/PA6 | 1805.1 | 50.1 | 154.6 | 104.5 |
| PC2–PPO/PA6/CNTs | 1866.1 | 64.5 | 161.6 | 97.1 |
| PC3–PPO/PA6/CNTs-COOH | 2157.1 | 71.7 | 161.1 | 89.4 |
| PC4–PPO/PA6/CNTs-OH | 2249.2 | 67.3 | 158.3 | 91.0 |
| PC5–PPO/PA6/CNTs-$NH_2$ | 2700.3 | 72.4 | 160.3 | 87.9 |

[a] Storage modulus of the composites at 0°C.

occurs between —OH and —COOH groups of the functionalized carbon nanotubes, which leads to compact aggregates of CNTs-COOH. In general, the state of dispersion of different CNTs is correlated to their structure, and particularly the polarity of the functional group attached on the CNT skeleton.

The state of dispersion of CNTs as well as their interaction with polymer matrix will influence the properties of the composites. Figure 5 shows the tensile test results of PPO/PA6(60/40) blends with different CNTs. All composites have a higher tensile modulus than that of the PPO/PA6(60/40) blend. However, the tensile strength decreased with most CNTs, except for pure CNTs which results in a very slight increase in tensile strength.

The strengthening mechanism of CNTs in polymer matrix has long been argued. Generally,[19] CNTs finely dispersed in the matrix with strong interaction between CNTs and the polymer will induce a strengthening effect. From Figure 4, it is proposed that pure CNTs are dispersed better than functionalized CNTs, resulting higher tensile modulus and higher tensile strength. Functionalization of CNTs leads to increased interaction between CNTs and the polymer matrix (especially with PA6, which has amide groups in chain segments), which increases the confinement effect of CNTs on polymer chains and thus increases the tensile modulus of the composites. However, CNTs are shortened during functionalization process, which decreases the strengthening effect of CNTs. Furthermore, the aggregations of CNTs-x behave like defects in the composites, inducing stress concentration and thus reducing the tensile strength of the composites.

Figure 6(a) shows the temperature dependence of the storage modulus ($E'$) of PPO/PA6(60/40)/CNTs-x. Two distinct decreases are observed from low temperature to high temperature in the curve, corresponding to the chain segment relaxation of PA6 and PPO, respectively. It is clear that the addition of CNTs-x increases the $E'$ of the blend, especially in the low temperature region. The effects of the different type of CNTs-x are varied to a similar extent as the tensile modulus, as shown in Figure 5(a).

Figure 6(b) shows the loss tangent (tan δ) verses temperature curve of the PPO/PA6(60/40)/CNTs-x composites. The peaks in the curve correspond to the glass transition temperatures ($T_g$) of the polymer

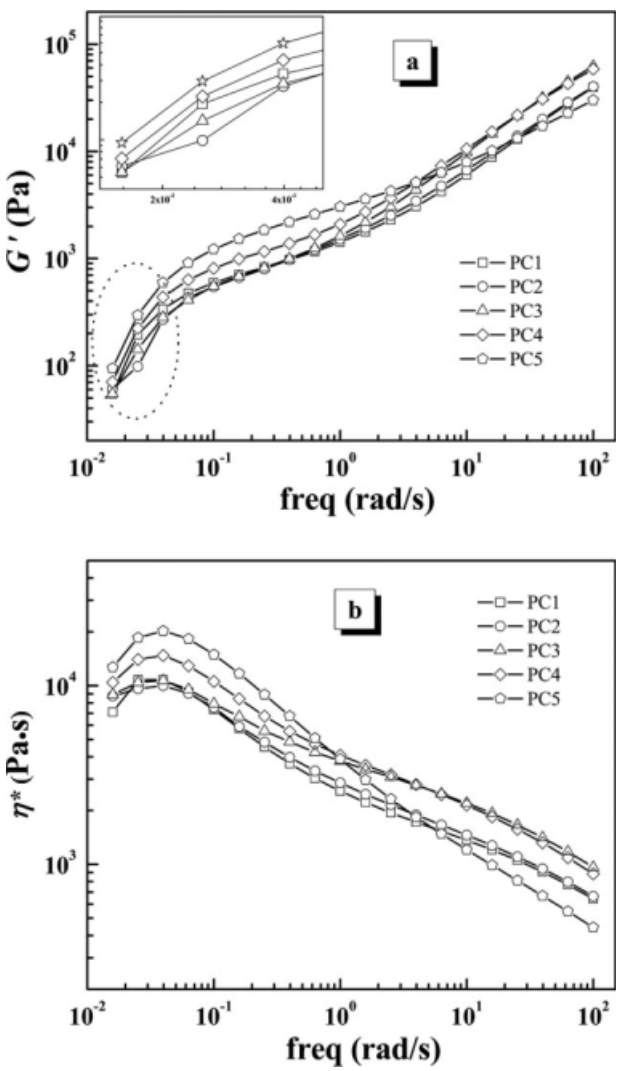


**Figure 7** Storage modulus ($G'$) and complex viscosity ($\eta^*$) of (PC1) PPO/PA6 (60/40), (PC2) PPO/PA6/pristine CNTs (60/40/1), (PC3) PPO/PA6/CNTs-COOH (60/40/1), (PC4) PPO/PA6/CNTs-OH (60/40/1), and (PC5) PPO/PA6/CNTs-$NH_2$ (60/40/1).

phases. Table I lists the $T_g$ values of the different samples. The $T_g$ of PA6 and PPO in PPO/PA6(60/40) binary blend are 50.1 and 154.6°C, respectively. Adding CNTs increases the glass transition temperatures of both PA6 and PPO, meanwhile, decreases the gap ($\Delta T_g$) between two glass transition temperatures. This is because CNTs, especially those that are functionalized, are located preferentially in PA6 phase, inducing the increment in $T_g$ of PA6 more significantly than that of PPO.

The storage modulus ($G'$) and complex viscosity ($\eta^*$) of the PPO/PA6(60/40)/CNTs-x composites versus the dynamic frequency sweeping is shown in Figure 7. At low frequencies, $G'$ and $\eta^*$ all increase with the addition of CNTs. Normally, higher $G'$ and $\eta^*$ values at low frequencies result in a slow relaxation of the entire macromolecular chain, i.e., chain motion is confined. The addition of CNTs changes the phase structure of the blend, as shown in Figure 3. Such a change leads to a sensitive response in the dynamic rheological behavior. For pure CNTs and CNTs-OH, the interaction between the tubes and polymer component is weak, hence the increment in $G'$ and $\eta^*$ values is not significant. The amino group in CNTs-$NH_2$ has strong interaction with the carboxyl group in PA6, leading to a strong confinement effect of CNTs-$NH_2$ to PA6 chains. Consequently, PPO/PA6(60/40)/CNTs-$NH_2$ has the highest $G'$ and $\eta^*$. Although the carboxyl group in CNTs-COOH could also have strong interaction with the amino group in PA6, the confinement effect of CNTs-COOH is not as strong as CNTs-$NH_2$, due to the compact aggregation of CNTs-COOH.

## CONCLUSIONS

Functional CNTs: CNTs-OH, CNTs-$NH_2$, and CNTs-COOH were obtained through the chemical modification of pristine CNTs. Different CNTs were introduced into a PPO/PA6 (60/40) blend via melt blending. The addition of CNTs, CNTs-OH, and CNTs-$NH_2$ resulted in the evolution of the phase morphology of PPO/PA6 (60/40) blend from sea-island to cocontinuous, while incorporating CNTs-COOH does not change the blend morphology due to significant aggregation of the CNTs. The presence of different CNTs considerably increases the tensile modulus and storage modulus, whereas slightly decreases the tensile strength of the PPO/PA6 blends. Consequently, the glass transition temperatures of PA6 and PPO are shifted to higher temperatures. $\Delta T_g$, the gap between the $T_g$ of PA6 and PPO, reduces with the addition of CNTs due to the stronger interaction of CNTs with PA6 than PPO, indicating an improvement in the compatibility of the blends. The state of dispersion of different CNTs and their interaction with polymer components are varied and thus cause a range of confinement effects within the polymer chains.

## References


1. Wang, X. D.; Feng, W.; Li, H. Q.; Jin, R. G. J Appl Polym Sci 2003, 88, 3110.
2. Dedecker, K.; Groeninckx, G. J Appl Polym Sci 1999, 73, 889.
3. Costa, D. A.; Oliveira, C. M. F. J Appl Polym Sci 2001, 81, 2556.
4. Wu, D. Z..; Wang, X. D.; Jin, R. G. Eur Polym J 2004, 40, 1223.
5. Ji, Y. L.; Ma, J. H.; Liang, B. R. Mater Lett 2005, 59, 1997.
6. Ji, Y. L.; Li, W. G.; Ma, J. H.; Liang, B. R. Macromol Rapid Commun 2005, 26, 116.
7. Ji, Y. L.; Ma, J. H.; Liang, B. R. Polym Bull 2005, 54, 109.
8. Li, Y. J.; Shimizu, H. Macromol Rapid Commun 2005, 26, 710.
9. Li, Y. J.; Shimizu, H. Polymer 2004, 45, 7381.
10. Li, B.; Zhang, Y.; Wang, S.; Ji, J. L. Eur Polym J 2009, 45, 2202.
11. Li, Z. M.; Li, S. N.; Xu, X. B.; Lu, A. Polym Plast Technol Eng 2007, 46, 129.
12. Li, Y. J.; Shimizu, H. Macromolecules 2008, 41, 5339.
13. Liu, L.; Wang, Y.; Li, Y. L.; Wu, J.; Xiang, F. M.; Zhou, Z. W. J Polym Sci Part B: Polym Phys 2009, 47, 1331.
14. Sui, G.; Zhong, W. H.; Ren, X.; Wang, X. Q.; Yang, X. P. Mater Chem Phys 2009, 115, 404.
15. Collister, J. Conference on Fine, Ultrafine and Nano Particles'00; Montreal, Quebec, Canada, 2000.
16. Tsang, S. C.; Chen, Y. K.; Harris, P. J. F.; Green, M. L. H. Nature 1994, 372, 159.
17. Liu, J.; Rinzler, A. G.; Dai, H.; Hafner, J. H.; Bradley, R. K.; Boul, P. J.; Lu, A.; Iverson, T.; Shellmov, K.; Huffman, C. B.; Rodriguez-Macias, F.; Shon, Y. S.; Lee, T. R.; Colbert, D. T.; Smalley, R. E. Science 1998, 280, 1253.
18. Meng, H.; Sui, G. X.; Fang, P. F.; Yang, R. Polymer 2008, 49, 610.
19. Zhang, W. D.; Shen, L.; Phang, I. L.; Liu, T. X. Macromolecules 2004, 37, 256.